

F.C. CHEONG¹
C.H. SOW^{1,2,✉}
A.T.S. WEE^{1,2}
P. SHAO^{1,3}
A.A. BETTIOL^{1,3}
J.A. VAN KAN^{1,3}
F. WATT^{1,2,3}

Optical travelator: transport and dynamic sorting of colloidal microspheres with an asymmetrical line optical tweezers

¹ Department of Physics, Blk S12, Faculty of Science, National University of Singapore,

2 Science Drive 3, Singapore 117542, Singapore

² National University of Singapore Nanoscience and Nanotechnology Initiative, 2 Science Drive 3, Singapore 117542, Singapore

³ Centre for Ion Beam Applications, Department of Physics, National University of Singapore, Blk S12, 2 Science Drive 3, Singapore 117542, Singapore

Received: 18 October 2005/Revised version: 6 January 2006
Published online: 8 February 2006 • © Springer-Verlag 2006

ABSTRACT We report the transport, funnelling and dynamic sorting of colloidal microspheres in an aqueous suspension using line optical tweezers with asymmetrical intensity profiles. The line tweezers readily trapped and propelled the microspheres along the length of the line tweezers. Using this simple technique, transporting and funnelling of microspheres within a microscopic region were demonstrated. To illustrate the dynamic particle-sorting capability of the line tweezers, a binary colloidal system comprising of microspheres with diameters of 1.1 μm and 3.2 μm were driven past the line tweezers by electrophoresis. As the optical trapping force is dependent on the size of the microspheres, the line tweezers was able to change the path of the larger spheres while exerting little influence on the smaller spheres thus sorting the two types of microspheres. At optimized laser power and flow rate of microspheres, sorting efficiency greater than 90% has been achieved.

PACS 42.15.Eq; 87.80.Cc; 87.80.Fe; 82.70.Dd

1 Introduction

The pioneering work of Ashkin et al. [1–3] in the invention of optical tweezers has provided us with an important tool in colloidal physics and biophysics [4–6]. In most cases, the optical tweezers are used to trap, manipulate and arrange tiny particles such as microspheres and biological cells. With the advent of optical tweezers, a wealth of interesting experiments has become feasible [6]. Among the many exciting applications of optical tweezers, sorting of microscopic particles in motion using light fields has been a subject of great interest [7]. With a single spot tweezers, it is straightforward to trap and re-direct a specific moving particle to a collection compartment during the sorting process [8]. Recently, optical manipulation and sorting has also been demonstrated with a diode laser bar to form a line trap that has a large trapping zone [9]. One could also make use of optical tweezers as actuators for a microscopic valve flap to direct micro-particles in a lab-on-a-chip device [10]. On the other hand, an array of optical traps has been demonstrated to be effective in deflecting the trajectory of driven particles [11]. This behavior is utilized

in a particle sorting technique known as optical fractionation [12, 13]. In these experiments, it is typical to orientate a regular array of optical traps [11] or a single array of optical traps [12, 13] at an inclined angle with respect to the flow direction of the driven particles. At the appropriate conditions, the trajectory of a specific type of driven particle is deflected by a trap and moves into the domain of the next trap and so on, while the remaining particles escape from the trap and flow away in the driven direction. In a recent development, MacDonald et al. [14] created a three-dimensional optical lattice from a five-beam interference pattern that facilitates sorting of particles by size and by refractive index. Unlike most conventional sorting techniques that operate on permanent embedded functionality structures [15, 16], sorting particles with light is non-invasive and free from the issue of clogging. The process can be dynamically optimized for better efficiency by adjusting the wavelength, intensity and geometry of the trap array.

In this work, we report an efficient way for transporting and sorting colloidal microspheres using a line optical tweezers with non-uniform intensity profile. The advantages of this technique are that it is simple to implement and relatively inexpensive. A line optical tweezers can be readily created by rapidly scanning a single spot optical tweezers using an acousto-optical modulator (AOM) [17] or a galvanometer [18]. Using a variation of the scanning technique with an AOM, Liesfeld et al. [19] created an asymmetrical line optical tweezers that was used to transport particles along the scanning-line optical tweezers [19]. Among the different methods used to create a line optical tweezers, perhaps the simplest and most cost effective method is to insert a cylindrical lens in the optical train of a typical optical tweezers system [20]. Such line tweezers has been used to align biological cells [20] and nanowires [21]. Similarly, we adopted the technique of using a cylindrical lens to create line optical tweezers. However, in this work, the main difference is that we have intentionally created a line optical tweezers with an asymmetric beam profile by inserting the cylindrical lens in a tilted and off-axis manner. The optical gradient force along the long axis of the asymmetrical line optical tweezers (length range from 1 mm to 100 μm) will translate one or more trapped microspheres along it readily. We denote this type of asymmetrical non-scanning line optical tweezers as an optical travelator since the microspheres travel readily along the line tweezers.

✉ Fax: +65-6777-6126, E-mail: physowch@nus.edu.sg

With two such optical travelators, we were able to demonstrate the efficient herding of a system of moving colloidal microspheres into a local area. This would otherwise be time consuming if one were to use a single spot optical tweezers. Finally, we use electrophoresis to drive a binary colloidal system comprising polystyrene microspheres with diameters of $1.1\ \mu\text{m}$ and $3.2\ \mu\text{m}$ through the optical travelator. With optimized flow direction (w.r.t. the optical travelator) and flow velocity, we sorted the larger spheres from the smaller spheres with a 90% or better efficiency.

2 Experimental setup

Figure 1a shows the schematic of the experimental setup used in this work. It is a typical setup for a dual beam optical tweezers system with cylindrical lenses (focal length: 19 mm) inserted in the laser beam paths to achieve a line tweezers with non-uniform intensity profile. Our sample consists of aqueous suspensions of negatively charged polystyrene or silica microspheres sealed between piranha etched cover glass and a glass slide (glass-to-glass separation $3\sim 10\ \mu\text{m}$) with access provided by two glass tubes bonded to holes passing through the upper glass wall. Clean glass and negatively charged colloidal particles will minimize the

probability of particles becoming trapped on the glass surfaces during the experiment. Two copper electrodes were introduced through these two glass tubes to provide an applied electric field to induce motion of the colloidal particles.

Once assembled, the sample was placed on the sample stage of an inverted Nikon TE300 microscope that was equipped with an oil-immersion objective lens ($100\times$, N.A. = 1.3). The transparent sample was illuminated in transmission mode with a halogen light source from the top. A Hamamatsu CCD camera was used to capture the images. The images were recorded onto videotapes or fed directly to a computer.

A SUWTech LDC-2500 diode laser, emitting laser beams at a wavelength of 1064 nm and a maximum power of 400 mW was utilized in this work. The laser beam was split into two separate paths by a beam splitter. Each beam path passes through a cylindrical lens before being recombined and directed through a lens and into the microscope through a side port. The beams were then reflected by a beam-splitter towards the objective lens. In this work, the laser beam was directed towards a tilted cylindrical lens in an off-axis manner as shown in Fig. 1. As a result, the laser spreads out into a line formation. As such, a portion of the line profile was blocked off at the back of the objective lens, and only the remaining portion that passed through the lens would be focused tightly onto the sample cell. To create flowing particles in the sample chamber, we used a Keithley 237 pico-ammeter to apply a voltage from 0 to 110 V to the copper electrodes embedded within the sample chamber. A uniform flow was established electro-kinetically by the applied electric field and with the velocity of the moving particles controlled by the magnitude of the applied voltage. Alternatively, we used a computer control x - y motorized sample stage to control the motion of the sample with respect to the line tweezers. Figure 1b shows a plot of the measured profile of the laser beam power after passing through a cylindrical lens. The profile was measured by attaching a slit with a width of about 2 mm in front of the detection window of a power meter and moving the power meter along the length of the expanded laser line. The region between the dashed lines was the part of the laser profile that was employed to form the line optical tweezers. In this way, the resultant line tweezers had non-uniform and monotonously increasing intensity profile. The microspheres were found to travel readily along the line tweezers towards the end with higher intensity. Since the strength of the optical trapping depends on the power of the laser beam, one can readily tune the trapping force by varying the power of the laser beam.

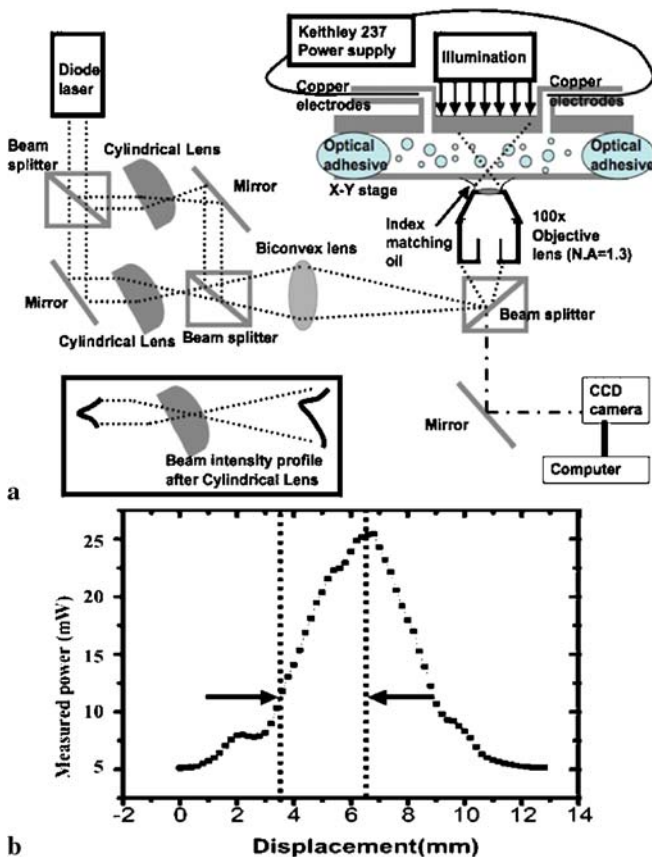


FIGURE 1 (a) shows a schematic of a double line optical tweezers system and a sample cell that was coupled with electrodes for electrophoresis. The inset shows the schematic of the intensity profile after a parallel beam with Gaussian intensity profile passes through the cylindrical lens resulting in the creation of a skewed intensity profile. (b) Measured laser power profile after passing through a cylindrical lens. The region bound by the dotted lines was focused by the objective lens to create the line optical tweezers

3 Results and discussions

3.1 Transportation and herding of colloidal microspheres

As a simple demonstration, the line optical tweezers was incident upon an aqueous suspension of silica microspheres with a diameter of $1.58\ \mu\text{m}$. Figure 2a shows the silica microspheres readily travelling along the line tweezers towards the end with a higher intensity profile. To better illustrate the sequence of events, video clips of the optical travelator in action can be found in the reference material [22]. In our work, the cylindrical lenses were mounted on a rotating optical mount. With proper alignment and centering, rotating the

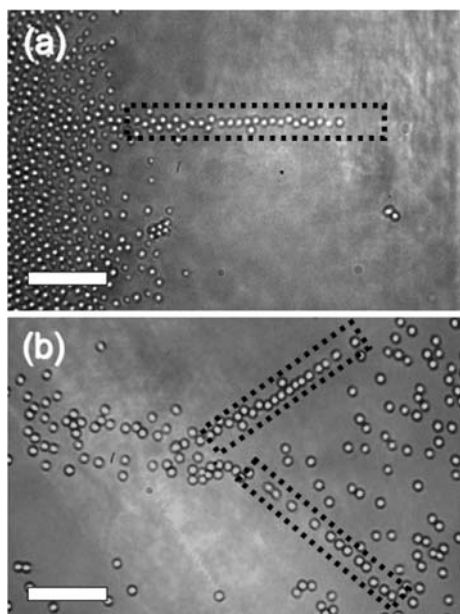


FIGURE 2 (a) Optical micrograph of a 2-D system comprising silica microspheres (diameter: $1.58\ \mu\text{m}$) under the influence of a single optical travelerator. (b) Optical micrograph showing herding of polystyrene microspheres (diameter: $1.2\ \mu\text{m}$) using two optical travelerators. The dotted line boxes outline the region where the optical travelerators affect the microspheres. Scale bars = $10\ \mu\text{m}$. Videoclips of the optical travelerator in action can be found in the supplementary material [22]

whole cylindrical lens resulted in rotation of the optical travelerators. With two optical travelerators, we could readily “herd” a system of colloidal microspheres and guide them towards a local area. As shown in Fig. 2b and supplementary material [22], two optical travelerators were orientated to form a “V” formation to redirect and gather a system of polystyrene microspheres (diameter $1.2\ \mu\text{m}$) towards a narrow region; the microspheres were made to travel generally from right to left by moving the sample stage. The “herding” of the microspheres was effective and efficient using such a combination of optical travelerators. To perform a similar task using a single spot optical tweezers would be less effective and efficient. One could envisage using this method to concentrate a system of particles towards a collection or compartment, and thereby reducing sample wastage.

3.2 Dynamic sorting of colloidal microspheres

The magnitude of the optical trapping force depends on the power of the laser beam, the refractive index difference of the dielectric particles compared to the medium, and the size of the particles. One could make use of these properties to sort moving particles by adjusting the magnitude of the optical trapping force to selectively deflect only the larger particles. In this work, we use the laminar flow caused by an applied electric field to drive a binary system of colloidal microspheres through a single optical travelerator. The diameters of the polystyrene microspheres were $1.1\ \mu\text{m}$ and $3.2\ \mu\text{m}$. In the following experiments, we kept the laser output power fixed at $400\ \text{mW}$ and systematically varied the applied voltage across the copper electrodes. As the optical trapping force was stronger for the larger microspheres, one can selectively de-

flect the larger particles without any significant effect on the smaller ones by controlling the flow rate. In this work, we have also varied the relative orientation between the optical travelerator and the direction of the flow of the microspheres.

Figure 3a is a photograph of the sample chamber showing both the large and small microspheres. The separation between the cover glass and the glass slide was found to be $5\ \mu\text{m}$. The microspheres flow from top to bottom of the field of view and the location of the optical travelerator is as indicated. We denote the angle between the particle flow vector and optical travelerator as θ (see Fig. 3a). The data presented in Fig. 3 correspond to the result obtained for $\theta = 74^\circ$. The process of optical sorting was recorded onto videotape or fed directly to the computer. The images were digitized and the centroid of the microspheres in each frame was identified. Joining the centroids of the microspheres over consecutive image frames give the trajectories of the microspheres. Figure 3b–d shows the trajectories of both the $3.2\ \mu\text{m}$ polystyrene microspheres (thick lines) and $1.1\ \mu\text{m}$ polystyrene microspheres (thin dotted lines) at applied voltages of Fig. 3b $10\ \text{V}$, Fig. 3c $50\ \text{V}$ and Fig. 3d $90\ \text{V}$, respectively. Changing the applied voltage varied the average drift velocity of the microspheres. The interplay between the momentum of the moving microspheres and the size-dependent trapping strength of the optical travelerator gave rise to three distinct phases of the system, namely,

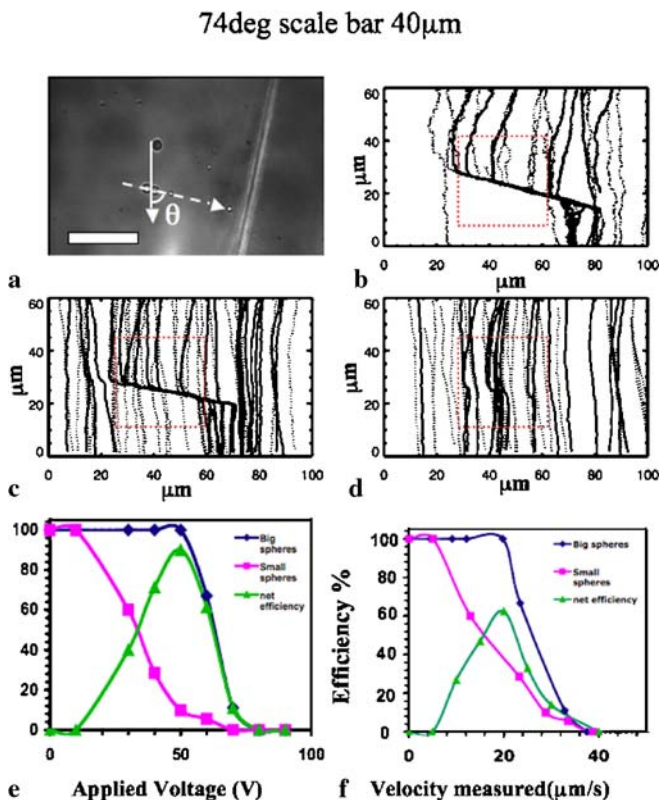


FIGURE 3 (a) Optical micrograph of the colloidal system. The arrows indicate the direction of flow of the particles and the direction of the optical travelerator. $\theta = 74^\circ$ and scale bar = $40\ \mu\text{m}$. Trajectories of the microspheres in the same region of flow for a binary system of $1.1\ \mu\text{m}$ (thin dotted line) and $3.2\ \mu\text{m}$ (thick lines) polystyrene spheres at an applied voltage of (b) $10\ \text{V}$, (c) $50\ \text{V}$ and (d) $90\ \text{V}$. (e) A plot of the particle deflections and net sorting efficiencies versus the applied voltage. (f) A plot of the particle deflections and net sorting efficiencies versus the measured velocity of the particles

the all-deflect phase at low particle velocity (Fig. 3b); sorting phase at medium particle velocity (Fig. 3c) and all-pass phase at high particles velocity (Fig. 3d). Videoclips of the optical sorting process can be found in the supplementary reference material [22].

At each applied voltage, the percentages of the larger microspheres and smaller microspheres deflected were obtained separately. The difference of the two percentages was taken to be the net efficiency of the sorting process. During the analysis, the selected region of interest was an area of $30\ \mu\text{m} \times 30\ \mu\text{m}$ as highlighted by red boxes in Fig. 3b–d. This region was selected to avoid the kink in the laser line profile as evident in Fig. 2a possibly due to a defect in the lens. A plot of the deflection and net efficiencies as a function of the applied voltage is shown in Fig. 3e. It can be seen that a maximum net efficiency of 90% was achieved at an applied voltage of about 50 V. The data shown were based on trajectories of more than 20 particles.

Electroosmosis and electrophoresis are major electro kinetic processes used in microfluidic applications. Electroosmosis refers to bulk motion of fluid and electrophoresis refers to the drift velocity of charged species by the action of an electric field. Due to electroosmosis flow, both types of microspheres would have almost the same velocity. As the charged microspheres are heavily screened by the counter ions in the solution, the effect of electrophoresis is not significant. The larger and heavier microspheres are expected to be closer to the lower glass wall where the velocity of the fluid flow is slower. This will result in a small difference in the average velocities of the two types of microspheres at the same applied voltage. From experimental measurement of the velocities of the two microspheres, we found that the averaged velocity of the $1.1\ \mu\text{m}$ -microspheres is about 1.3 times faster than the $3.2\ \mu\text{m}$ -microspheres within the same region of interest. Figure 3f shows a plot of the deflection and net efficiencies as a function of the measured velocity of the microspheres. It is evident that the maximum net efficiency as a function of microspheres velocity was about 60%. Hence, the applied voltage that provided the driving force to propel the microspheres also added an important velocity difference in the microspheres for better sorting efficiency.

One could also estimate the magnitude of the trapping force of the optical line tweezers in the direction orthogonal to the direction of motion of the spheres along the optical travelator. For example, from Fig. 3f, the big microspheres typical flow at a maximum speed of about $20\ \mu\text{m/s}$ at 100% deflection. The force required to keep the larger microspheres along the line tweezers while resisting the background fluid flow of $v = 20\ \mu\text{m/s}$ can be estimated as $F = 6\pi\eta r v \cos(16^\circ) = 0.58\ \text{pN}$, where $\eta (= 0.001002\ \text{Ns/m}^2)$ is the viscosity of water, $r (= 1.6\ \mu\text{m})$ is the radius of the microspheres.

The performance of the sorting capability of the optical travelator at different θ was also investigated. The different relative orientations were achieved by carefully rotating the sample chamber on the sample stage without disturbing the optical alignment of the system. We ensured that even after rotation, the region of interest remained the same by using permanent features on the glass slide as reference points. Figure 4 shows the results obtained at $\theta = 40^\circ$. It should be noted that the camera was rotated in order to achieve a view where the di-

rection of the flowing particles were from bottom to top of the field of view as shown in Fig. 4a. The polarity of the applied voltage was reversed so that the direction of motion of the microspheres was opposite to those shown in Fig. 3. Figure 4b–d shows the trajectories of the two types of microspheres at applied voltages of Fig. 4b 5 V, Fig. 4c 50 V and Fig. 4d 90 V. They correspond to the all-deflect phase at low particle velocity; sorting phase at medium particle velocity and all-pass phase at high particle velocity, respectively. Figure 4e shows a plot of the deflection and net efficiencies as a function of the applied voltage. It can be seen that a maximum net efficiency of 77% was achieved at an applied voltage of about 30–40 V. Evidently this maximum efficiency was less than that achieved at $\theta = 74^\circ$.

The dependence of the maximum net efficiency on the angle θ was systematically investigated by repeating the experiment at different θ . Figure 5 shows a plot of the maximum net efficiency (from efficiency versus voltage plot) versus the angle θ . It can be seen that effective sorting can be achieved at a range of $40^\circ < \theta < 74^\circ$. In this range, the moving large microspheres become effectively trapped by the optical travelator and propelled along the optical travelator while the majority of the smaller microspheres do not experience a sufficiently large trapping force to cause a large deviation in their

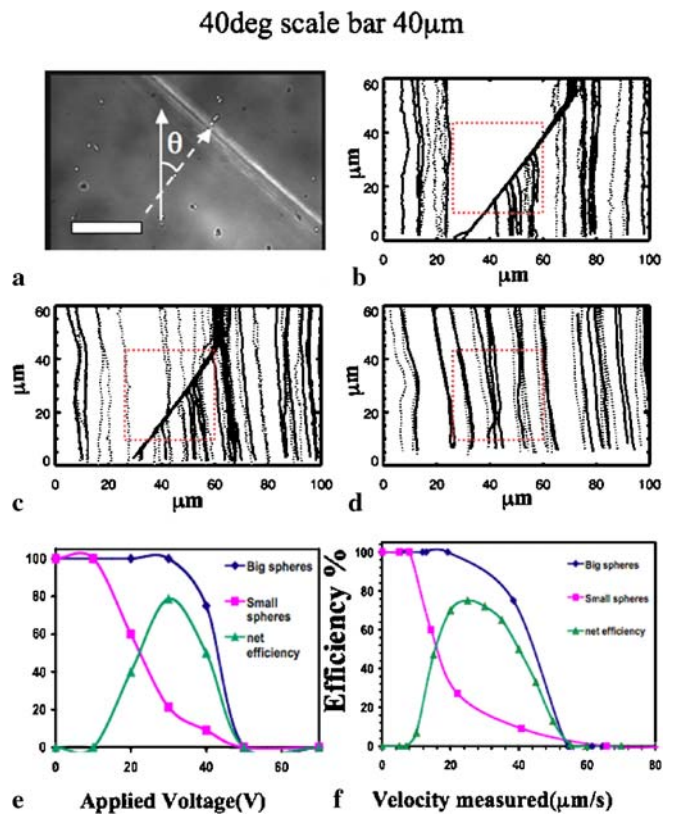


FIGURE 4 (a) Optical micrograph of a snapshot of the colloidal system. The arrows indicate the direction of flow of the particles and the direction of the optical travelator. $\theta = 40^\circ$ and scale bar = $40\ \mu\text{m}$. Trajectories of the microspheres in the same region of flow for a binary system of $1.1\ \mu\text{m}$ (*thin dotted line*) and $3.2\ \mu\text{m}$ (*thick lines*) polystyrene spheres at an applied voltage of (b) 5 V, (c) 50 V and (d) 90 V. (e) A plot of the particle deflection and net sorting efficiencies versus the applied voltage. (f) A plot of the particle deflection and net sorting efficiencies versus the measured velocity of the particles

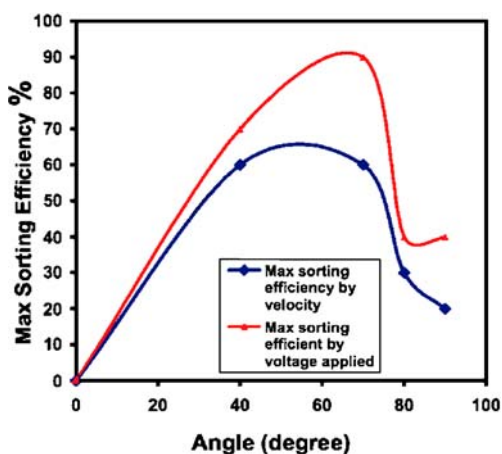


FIGURE 5 Maximum net efficiency versus θ

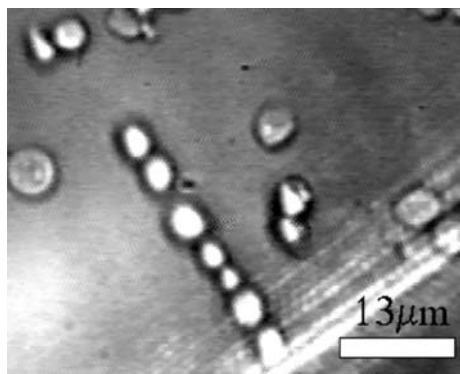


FIGURE 6 Optical micrograph of yeast cells trapped and transported using the optical travelators

trajectory. It should be noted that the force that propels the large microspheres along the optical travelator is due to a combination of optical force exerted by intensity gradient along the line tweezers, and the components of the viscous force exerted by the moving fluid. On the other hand, at angle of $\theta \geq 80^\circ$, the large microspheres become trapped by the line tweezers but do not travel fast enough along the travelator that they are knocked out of the travelator due to collisions with the next incoming microspheres. As a result, the sorting efficiency is reduced. With a reduced concentration of colloidal microspheres, the sorting efficiency at these large angles can be improved due to a reduction of collision frequency. This issue of the sorting efficiency with respect to the concentration of the microspheres in the colloidal system will be addressed in future experiments.

As a demonstration of manipulation of biological samples using this technique, we have applied the optical travelator on

yeast cells. The yeast cells lined up according to the line optical tweezers profile are driven towards the direction of the higher intensity laser profile as shown in Fig. 6. The video clip of the translation motion of yeast cells by the optical travelator can also be found in supplementary reference material [22]. This technique can be an alternative tool for manipulation of biological cells.

4 Conclusion

We have demonstrated the feasibility of using a line optical tweezers with asymmetrical intensity profile for the purposes of transportation, manipulation and sorting of microscopic particles. The technique is relatively inexpensive and easy to implement. It is useful as a possible alternative method using light fields for sorting of particles.

ACKNOWLEDGEMENTS CHS acknowledges the support of the Academic Research Fund from the National University of Singapore.

REFERENCES

- 1 A. Ashkin, Phys. Rev. Lett. **24**, 156 (1970)
- 2 A. Ashkin, J.M. Dziedzic, J.E. Bjorkholm, S. Chu, Opt. Lett. **11**, 288 (1986)
- 3 A. Ashkin, J.M. Dziedzic, Science **235**, 1517 (1987)
- 4 M.P. Sheetz (Ed.), *Laser Tweezers in Cell Biology* (Academic Press, San Diego, California 1998)
- 5 K. Svoboda, S.M. Block, Annu. Rev. Biophys. Biomol. Struct. **23**, 247 (1994)
- 6 D. Grier, Nature **424**, 810 (2003)
- 7 J. Gluckstad, Nature Materials **3**, 9 (2004)
- 8 M. Ozkan, M. Wang, C. Ozkan, R. Flynn, A. Birkbeck, S. Esener, Biomedical Microdevices **5:1**, 61 (2003)
- 9 R.W. Applegate Jr., Jeff Squier, T. Vestad, J. Oakey, D.W.M. Marr, Opt. Express **12**, 4390 (2004)
- 10 A. Terray, J. Oakey, D.W.M. Marr, Appl. Phys. Lett. **81**, 1555 (2002)
- 11 P.T. Korda, M.B. Talyor, D.G. Grier, Phys. Rev. Lett. **89**, 128301 (2002)
- 12 K. Ladavac, K. Kasza, D.G. Grier, Phys. Rev. E **70**, 010901 (2004)
- 13 M. Pelton, K. Ladavac, D.G. Grier, Phys. Rev. E **70**, 031108 (2004)
- 14 M.P. MacDonald, G.C. Spalding, K. Dholakia, Nature **426**, 421 (2003)
- 15 M. Cabodi, Y.F. Chen, S.W.P. Turner, H.G. Craighead, R.H. Austin, Electrophoresis **23**, 3496 (2002)
- 16 L.R. Huang, E.C. Cox, R.H. Austin, J.C. Sturm, Science **304**, 987 (2004)
- 17 R. Nambiar, J.C. Meiners, Opt. Lett. **27**, 836 (2002)
- 18 J.C. Crocker, J.A. Matteo, A.D. Dinsmore, A.G. Yodh, Phys. Rev. Lett. **82**, 4352 (1999)
- 19 B. Liesfeld, R. Nambiar, J.C. Meiners, Phys. Rev. E **68**, 051907 (2003)
- 20 R. Dasgupta, S.K. Mohanty, P.K. Gupta, Biotechnol. Lett. **25**, 1625 (2003)
- 21 T. Yu, F.C. Cheong, C.H. Sow, Nanotechnology **15**, 1732 (2004)
- 22 Video clips of the optical travelator in action can be found in the following website http://www.physics.nus.edu.sg/~physowch/optical_travelator/optic_travelator.html